RESPONSE TO AN IONOSPHERIC PERTURBATION AT HF: RESULTS FROM SIMULTANEOUS SIX-BAND WB6CXC *'BEACON BLASTER-6'* FST4W TRANSMISSIONS DURING THE 11 JULY 2023 R2 BLACKOUT OVER N. AMERICA

Key findings

- The usefulness of a digital-modes, six-band, simultaneous trans-missions, 100% duty cycle HF beacon for observing ionospheric perturbations has been demonstrated.
- The specification may seem overkill, but the full capability was needed to delineate excess D layer absorption following an M6 solar flare. Predictable band conditions meant 3.5 MHz was closed. Unpredictable conditions, possibly sporadic E, affected 21 MHz. 28 MHz had too few decodes. Peak absorption, taken with prevailing signal to noise ratio, meant only partial delineation at 7 MHz and 14 MHz. This left one band out of six, 10 MHz, with a full picture of the absorption event.
- An output power of 5 W (37 dBm) rather than 1 W (30 dBm) would have provided a complete picture at 14 MHz at KPH but not at 7 MHz.
- Transmissions every two minutes proved essential. First, some decodes were missed; their loss would have had greater impact if the duty cycle was not 100%. Second, 100% duty cycle gave just sufficient time resolution to show absorption event asymmetry of onset and decay.
- SNR is not a good proxy for signal level when signal and noise levels co-vary. That happens at sites limited by propagated-in noise. Measuring noise at the same time and frequency with WsprDaemon allows signal levels to be calculated.
- Using FST4W as the digital mode, with its measurement of frequency spread, shows one-hop propagation to occur as excess absorption suppressed otherwise co-occurring two-hop propagation.
- The observed oblique path absorption at 10 MHz was 7 dB greater than an estimate from applying Martyn's theorem to the vertical absorption NOAA/SWPC model. This discrepancy is in line with many professional studies.

1. Introduction

Paul Elliott WB6CXC has developed the 'Beacon Blaster-6' able to transmit FSK digital modes simultaneously on six HF bands with up to 100% duty cycle [1]. Available from Turn Island Systems the 'Beacon Blaster-6' was conceived as a contribution to the 14 October 2023 and 8 April 2024 HamSci Festivals of Eclipse Ionospheric Science [2]. 'Beacon Blaster-6' prototypes have been tested extensively on the bench and over the air. This article reports on a usability test, with multiple receivers, during a short-lived perturbation to the ionosphere.

X-ray emissions from an M6 solar flare at 18:08 UTC on 11 July 2023 provided a strong perturbation to the ionosphere, although of a very different kind to an eclipse. Nevertheless, the perturbation provided a valuable and fascinating testing and learning opportunity. A solar flare-induced blackout, **Figure 1**:

- Affects the sunlit side of the Earth over most of its area.
- Is caused by X-ray bombardment greatly enhancing the electron density in the D layer causing increased absorption [3].
- Has a depth (excess absorption) that depends on the number of times a signal passes through the D layer, that is, on the number of hops.
- Has greatest impact at lower frequencies (< 5 MHz) but affects the entire HF band.
- Lasts around 40 minutes.

The map and graph in **Figure 1** from a NOAA/SWPC model of the 11 July 2023 event [4] shows:

1. The timing meant continental North America was affected in its entirety, including the path from the West Coast to Maui.
2. The intensity from the model was sufficient to result in 5 dB excess absorption at 14 MHz and 13 dB at 7 MHz *per vertical transition* through the D layer.

These two features meant that the event was an excellent test, and investigative application, for the *'Beacon Blaster-6'* transmitter and the US network of KiwiSDR FST4W receivers. This paper is organised as follows: section 2 outlines the equipment and measurements; section 3 lists summary statistics of data return and propagation paths; section 4 presents noise levels changes at key sites; section 5 presents estimates of the oblique path

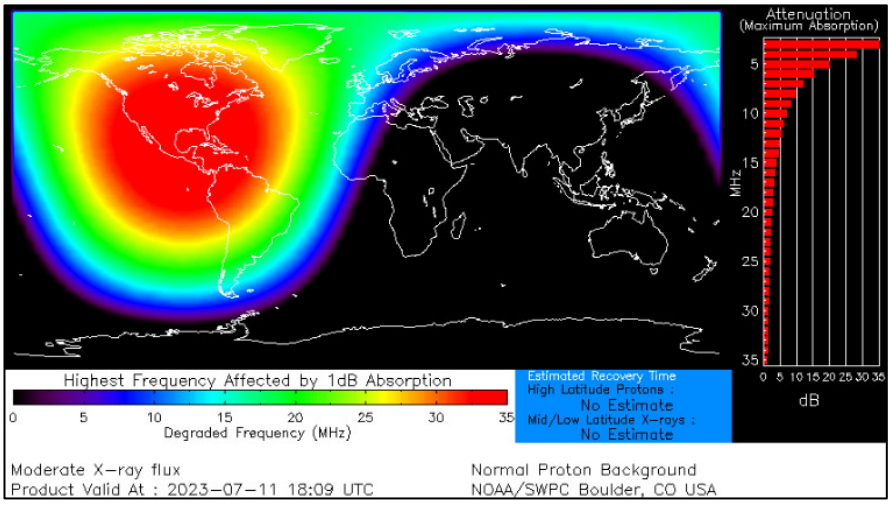

Figure 1. Excess ionospheric absorption following an X-ray burst from a model by NOAA/SWPC for 18:09 UTC on 11 July 2023 The map shows the absorption event covered entire North America the graph at right shows the pattern of excess absorption with frequency from the model.

excess absorption, section 6 looks at frequency spread to see how the number of hops changed during the event, section 7 compares model and observed excess absorption at 10 MHz.

2. Methods

2.1 Turn Island Systems 'Beacon-Blaster-6' transmitter

The *'Beacon Blaster-6'*, **Figure 2**, is a transmitter that generates FSK signals on six bands simultaneously - in this study FST4W-120. It does so using two Si5351 programmable clock generators, each of which generates three independent output frequencies. The frequency range is 1.8 MHz to 50 MHz. Each Si5351 channel is fed to an identical, separate, 1 W Class D amplifier with square-wave output. Single-channel low pass filters follow. The outputs of up to four channels with octave separation can be routed to a passive combiner, e.g. for 3.5, 7, 14 and 28 MHz. This produces a single output for simultaneous transmissions using a multiband antenna. The other two outputs, e.g. 10 and 21 MHz may be fed to another octave combiner or output to individual antennas.

To assure stability the transmit frequency is derived from a high-quality GPSDO (e.g. from Bodnar Electronics) or from an OCXO. Care has been taken to transmit FSK tones having sub-milliHz accuracy. Where some other beacons use unfiltered FSK (as specified in WSPR), the *'Beacon Blaster-6'* generates Gaussian Frequency Shift FSK using DSP techniques, as specified for FST4W. (The degree to which this matters in practice has yet to be established.)

For this experiment the *'Beacon Blaster-6'* was operated by WB6CXC from Friday Harbour, WA., grid square CN88.

2.2 Receivers

The receivers for this study needed to be receiving FST4W-120 on the HF bands reporting frequency spread [5] and local noise to the WsprDaemon database [6]. The 12 KiwiSDR sites shown in **Figure 3** met these criteria and decoded sufficient transmissions from the *'Beacon Blaster-6'* to be useful in these studies (KPH is hidden on the map). Other KiwiSDR sites in the US did decode some transmissions but not enough to analyze.

Band (MHz)	No. reports from:		No. of Decodes	No. of useful:	
	Sites	Receivers		Sites	Receivers
3.5	1	1	1	0	0
7	6	9	241	6	8
10	10	15	708	9	14
14	16	28	765	8	13
21	9	13	275	4	6
28	4	5	55	0	0

Table 1. Summary statistics of the number of receiver sites and receivers with at least one decode on a band, the total number of decodes per band, and the subset of sites and receivers with sufficient decodes between 17:00 and 19:00 UTC on 11 July 2023 to be useful for analysis.

2.3 Measurements

Three measurements were required from each decode for this experiment:

1. Signal to noise ratio (SNR) - for FST4W the calculations are made within the jt9 program and its sub-programs within WSJT-X. The algorithm is different to that in WSPR. Ryan Tolboom, N2BP, has explained and annotated the relevant code in a blog post [7].
2. Frequency spread - adding an empty file with the name *plotspec* to the directory in which WSJT-X is run enables this optional measurement. Frequency spread increases with the number of hops. It helps us determine how many times the signal passed through the D layer.
3. Noise level - at sites where the noise level was limited by the propagated-in noise the solar-flare-induced blackout will also affect the noise level. Therefore we use the noise level and SNR to estimate signal level, being the truer parameter for this study.

Figure 2. The 'Beacon-Blaster-6' prototype #2 from Turn Island Systems, capable of simultaneous FSK transmissions on six bands from 1.8 MHz to 50 MHz. Image from https://turnislandsystems.com/beaconblaster-progress/

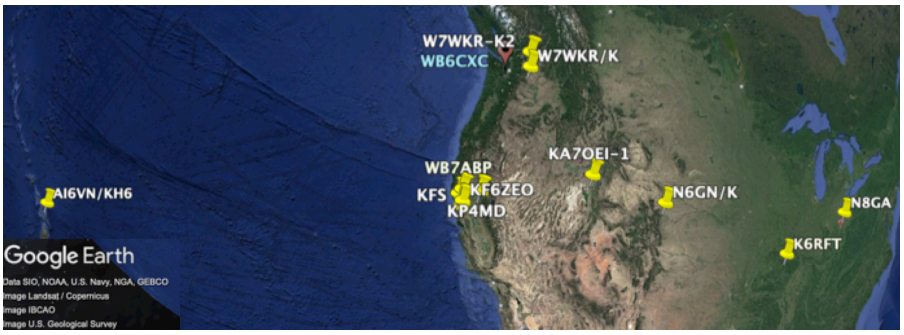

Figure 3. Map showing the transmitter site at WB6CXC, Friday Harbour, WA. and the KiwiSDR receiver sites with useful data on one or more bands. The marker for KPH in the San Francisco Bay area is hidden.

Band (MHz)	Site	Path (km)	Receiver	Baseline SNR (dB)	No. Hops	Model absorption (db/transit)
7	KA7OEI-1	1137	NUT_KIWI2	-20.9	2	12
			NUT_KIWI4	-25.8		
	KFS	1234	KIWI_NW	-19.7	2	
			KIWI_Omni_C	-23.0		
	KP4MD	1098	KIWI_0	-27.3	2	
	KPH	1154	KPH_HF_76	-15.9	2	
	W7WKR-K2	173	KIWI_0	-10.7	1	
	W7WKR/K	238	KIWI_0	-10.6	1	
10	AI6VN/KH6	4265	maui76	-19.9	3	7
	KA7OEI-1	1137	NUT_KIWI1	2.6	1	
			NUT_KIWI5	-11.8		
			NUT_KIWI6	4.2		
	KF6ZEO	1196	KIWI_0	-21.8	1	
	KFS	1234	KIWI_NW	-5.9	1	
			KIWI_Omni_C	-3.2		
			KIWI_SE	-15.2		
			KIWI_SW	-9.5		
	KP4MD	1098	KIWI_0	-14.9	1	
	KPH	1154	KPH_HF_76	5.0	1	
	N6GN/K	1657	GN2	-21.2	1*	
	WB7ABP/K	1117	WB7ABP	-22.5	1	
14	AI6VN/KH6	4265	maui76	-9.9	2*	5
	K6RFT	2803	KIWI_0	-15.6	2	
	KA7OEI-1	1137	NUT_KIWI2	-16.0	1	
			NUT_KIWI4	-20.9		
			NUT_KIWI6	-9.0		
	KFS	1234	KIWI_NW	-20.2	1	
			KIWI_Omni_C	-11.9		
			KIWI_SE	-25.9		
			KIWI_SW	-22.0		
	KP4MD	1098	KIWI_0	-22.8	1	
	KPH	1154	KPH_HF_76	-2.2	1	
	N6GN/K	1657	GN2	-12.1	1	
	N8GA	3228	KIWI_1	-17.6	1*	
	WB7ABP/K	1117	WB7ABP	-28.0	1	
21	KA7OEI-1	1137	NUT_KIWI1	-2.9	1	2
			NUT_KIWI4	-9.5		
			NUT_KIWI6	-7.7		
	KFS	1234	KIWI_Omni_C	-24.1	1	
	KPH	1154	KPH_HF_76	-19.4	1	
	N6GN/K	1657	GN2	-18.1	1	

*Table 2. Summary of the sites and individual receivers that decoded enough FST4W-120 transmissions from WB6CXC to be useful in assessing excess absorption or showing the impact of insufficient baseline SNR. Entries with a * show the likely number of hops during the blackout although modes with more hops likely co-existed prior to, and after, the event. On 21 MHz all the paths were assumed to be one-hop, despite ray tracing showing the skip zone extending to 2500 km. Baseline SNRs shaded red meant it was unlikely that those receivers would have sufficient reserve of SNR to show the full depth of the absorption event.*

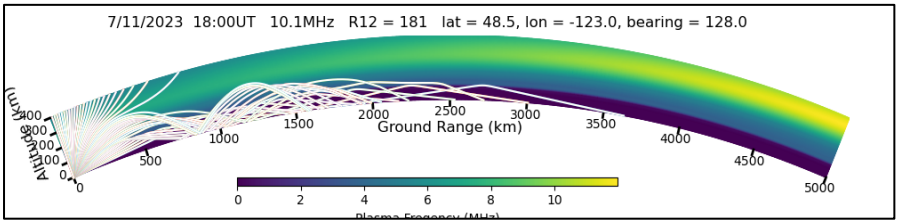

Figure 4. Ray trace for the 1657 km path from WB6CXC, Friday Harbour, WA. to N6GN/K near Fort Collins, CO. from PyLap showing the co-existence of one-hop and two-hop propagation at 18:00 UTC on 10 MHz, a situation likely applicable before and after the blackout.

2.3 Database

All of the KiwiSDRs reported their results to the WsprDaemon extended spots database, where the frequency spread is reported as the field 'metric' in milliHertz. The data is openly available [6].

3. Results: Data return

Our observation period for the event at 18:08 UTC on 11 July 2023 spanned 17:00 to 19:00 UTC. A key step in data analysis was to use the arithmetic average of properties (noise, SNR, signal level) before the event, from 17:00 to 17:30 UTC, as the baseline to subtract from the observations to derive anomalies. This step brought the individual receiver results to a common baseline.

Table 1 summarizes the data return and key metrics for this experiment. Of the total number of sites and receivers (some sites have more than one receiver) that decoded FST4W transmissions from WB6CXC several decoded too few to be useful for excess absorption analysis. The 3.5 MHz and 28 MHz bands had insufficient decodes for any analysis.

We need insight into the number of hops for each path as excess absorption happens on each transit through the ionosphere. Here, ray tracing was a useful tool. The PyLap implementation [8] of the PHaRLAP model was run for each path and frequency, **Table 2**. The model showed one-hop or two-hop propagation, exclusively, to be likely on most paths. However, on some paths both one-hop and two-hop could co-exist: for example on the WB6CXC to N6GN/K path at 10 MHz at a ground range of 1657 km, **Figure 4**. As we will see in section 6 FST4W frequency spread prior to the blackout was consistent with both propagation modes coexisting. However, during the event the expectation would be that one-hop would dominate, given the two-hop mode would be subject to twice the excess absorption. FST4W frequency spread measurements during the event lets us test this hypothesis.

4. Results: Noise level

At sites where the propagated noise was above the local noise excess absorption in the D layer would have reduced the level of propagated-in noise. At those sites SNR conflates two variables that change: the wanted signal level change and the noise level change. WsprDaemon measures

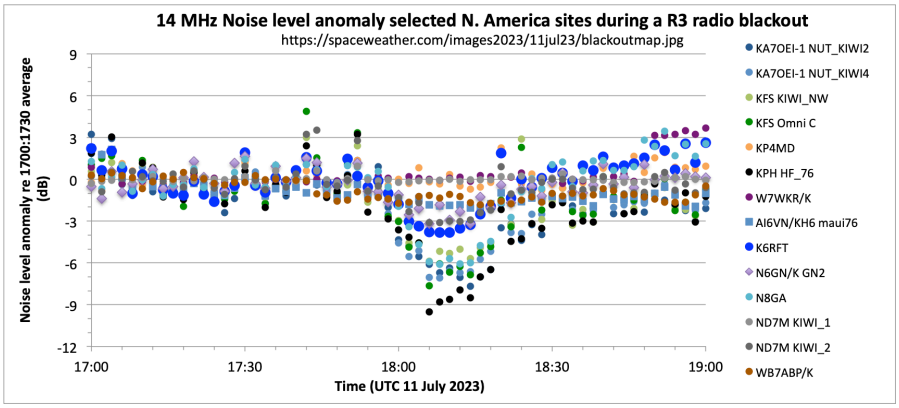

Figure 5. Noise level anomalies, calculated as differences from the mean at each receiver between 17:00 and 17:30 UTC. The deep dips were at those sites with low local noise. No dip is seen at those stations where the noise level was dominated by local rather than propagated-in noise.

noise level at the receiver enabling us to calculate signal level. Here we show noise level changes for one band, 14 MHz. Noise measurements have been used to derive signal level on all bands for the results in section 5.

Several KiwiSDRs in North America are at sites with low local noise [including, among others: KPH, KFS, the Northern Utah SDR site (NUT, KA7OEI-1), N6GN/K, K6RFT, N8GA]. At these sites daytime 14 MHz noise is dominated by that propagated-in from distance sources. Unfortunately, different antenna and RF distribution systems mean that quantitative comparison of as-recorded noise levels across the sites is not useful. However, we can look at noise anomalies.

To calculate anomalies we subtract mean noise level between 17:00 and 17:30 UTC, before the event, from the noise levels at two-minute intervals from 17:00 to 19:00 UTC. **Figure 5** shows the resulting time series for selected stations and receivers. The selection includes six sites with low local noise noted above, four typical amateur sites [KP4MD, W7WRK/K, ND7M and WB7ABP/K] and AI6VN/KH6, on Maui, at the edge of the affected region. No smoothing has been applied.

KPH, KFS (Omni_C and NW), NUT (KIWI2 and KIWI4), and N8GA showed a dip of 5 dB to 9 dB in noise level. Other sites showed a smaller dip: K6RFT, Houston Missouri, with 4 dB, and about 3 dB at N6GN/K and ND7M KIWI_2. There was a dip of about 2 dB at AI6VN/KH6, at the western edge of the affected region. **Figure 5** also shows sites where anomalies of 2 dB or less could have been due to changes *not* associated with the absorption event: at KP4MD, W7WRK/K, ND7M KIWI_1 and WB7ABP/K. At these sites local noise likely dominated.

5. Measurements of excess absorption

First we show results at the intermediate stages of SNR and SNR anomalies for 7 MHz, the lowest band with sufficient decodes. Second, we show the signal level anomalies for 7 MHz to 21 MHz, highlighting the solar flare induced excess absorption and other causes of changes in signal level.

5.1 From SNR to signal level anomalies on 7 MHz

The raw SNR for 7 MHz, **Figure 6**, shows a large spread between sites, this is only to be expected. Path length matters: the highest pre-event SNRs were at W7WKR-K2, at 173 km the closest site to the transmitter. Low noise matters: the SNR is some 15 dB higher at KPH than at KP4MD, a typical suburban amateur site at a similar range.

After the event there were fewer sites reporting, and fewer decodes from those sites that did. The likely explanation may be the combined effect of a reducing tail of excess absorption and normal diurnal D layer absorption as the time approached local noon (about 20:00 UTC).

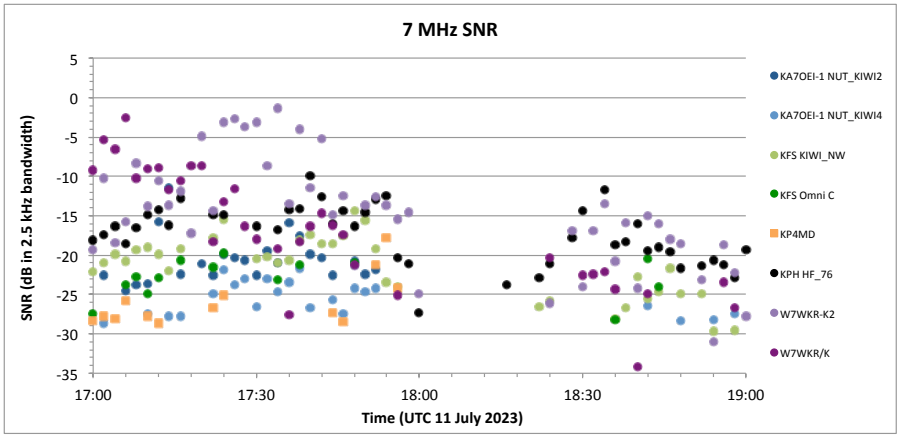

Figure 6. SNR on 7 MHz for WB6CXC FST4W-120 transmissions from CN88 for a selection of KiwiSDR sites from 173 km (W7WKR-K2) to 1137 km (KA7OEI-1).

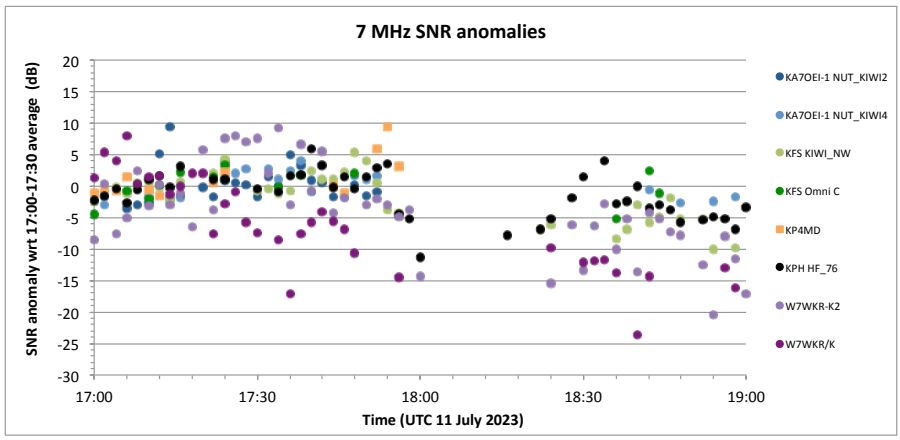

Figure 7. SNR anomalies on 7 MHz for WB6CXC FST4W-120 transmissions from CN88 for a selection of KiwiSDR sites, calculated as differences from the average SNR between 17:00 and 17:30 UTC.

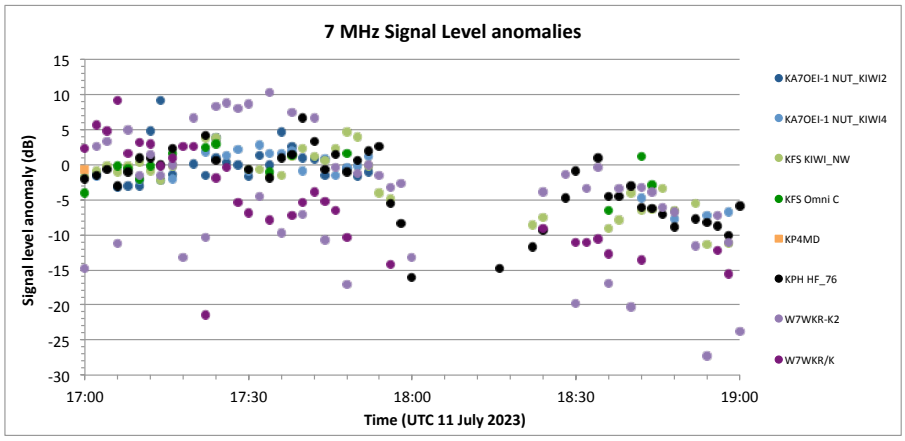

Figure 8. Signal level anomalies on 7 MHz for WB6CXC FST4W-120 transmissions from CN88 for a selection of KiwiSDR sites between 17:00 and 17:30 UTC, calculated from SNR and noise level as measured by WsprDaemon

No site decoded 7 MHz transmissions between 18:02 and 18:14 UTC inclusive. Only KPH had sufficient SNR to decode transmissions at both 18:00 and 18:16 UTC, going into, and coming out of, the dip. The implication is that the prevailing SNR at all these sites at 7 MHz, in the absence of the blackout, was insufficient for measurements to be made to the bottom of the excess absorption dip. While there is clear evidence of the blackout, we cannot determine the absorption, or its time history, on 7 MHz between 18:02 and 18:14 UTC.

Range- and site-dependent SNR variation can be removed by calculating SNR anomalies, **Figure 7**. Because of scatter in the W7WKR-K2 data, and insufficient SNR at other sites, the most convincing SNR anomalies, and only for the early and latter stages of the blackout, come from KPH with -5 dB at 17:58, -11 dB at 18:00 UTC, and -8 dB at 18:16.

We make the important step of moving beyond SNR anomalies by calculating signal level anomalies from SNR and noise level as measured by WsprDaemon, **Figure 8**. For KPH the SNR anomalies either side of the dip of -11 dB at 18:00 UTC, and -8 dB at 18:16 become signal level anomalies of -16 dB and -15 dB. These figures better represent the true excess absorption at the shoulder times on this 1154 km oblique path.

5.2 Signal level anomalies on 10, 14 and 21 MHz

Having followed the same procedure as for 7 MHz **Figures 9a-c** show the signal level anomalies, equating to oblique path excess absorption, for 10, 14 and 21 MHz. The measurements on 10 MHz were the most complete. The bottom of the dip is seen at KPH at 18:06 UTC with an excess absorption of 28.5 dB. Northern Utah KA7OEI-1 receivers KIWI1 and KIWI6 also recorded at the time of maximum dip, but the receivers at KFS did not. Of the more typical amateur sites KP4MD did best.

The 10 MHz plot shows the asymmetry of the event: rapid onset followed by a slower return to normal. This is in keeping with the intensity profile of a typical X-ray solar flare event.

The picture at 14 MHz is not so complete, **Figure 9b**. One reason is that, despite lower absorption than at 10 MHz

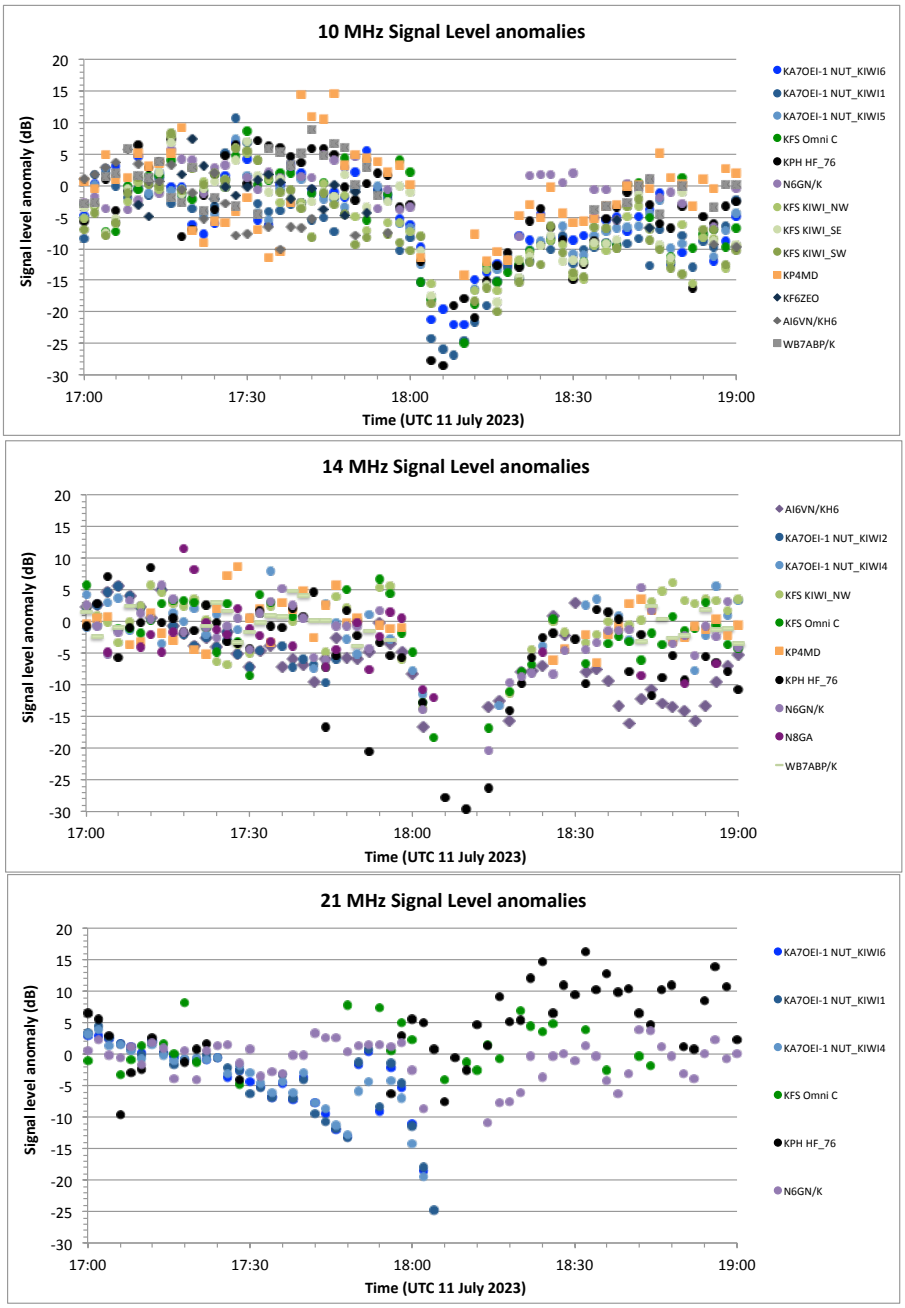

Figure 9. Signal level anomalies at, from top: a) 10 MHz, b) 14 MHz and c) 21 MHz. The most complete record was at 10 MHz.

(**Table 1**), the pre-event SNR was lower. KPH again observed the maximum absorption, 29.7 dB, although interestingly at 18:10 and not 18:06 UTC as at 10 MHz. Note that KPH did not decode the transmission at 18:08 UTC. The asymmetry of onset and recovery was not so clear-cut as at 10 MHz.

The results at 21 MHz were in complete contrast to the lower frequency bands, **Figure 9c**. These results are a mystery. PyLap ray tracing, based on monthly mean data, showed that, at that time of day, the skip zone at 21 MHz should have extended to 2500 km, encompassing all the receivers in this plot. Ionosonde records at Pt. Arguello, CA., and the Idaho National Laboratory showed F2 layer critical frequencies no higher than 9.0 and 7.2 MHz respectively. Neither showed blanketing E layers.

It is most curious that the three receivers at the Northern Utah site were the only ones to show a dip as the event began, reaching 24.7 dB at 18:04 UTC on KIWI4, but then not decoding at all during the recovery. There may be an argument that the higher signal levels during and after the event were because the band started to open, but that would also apply on the Northern Utah path. Speculatively, there may have been sporadic E propagation on the path from WB6CXC, Friday Harbour, WA., to the south, selectively favouring KFS and KPH. These are matters for further investigation.

6. Frequency spread variations during the blackout

The effect of the excess absorption event on frequency spread was best observed at 10 MHz and for the sites at 1137 km to 1234 km range [NUT KIWI1, KFS Omni_C, KFS NW, KPH HF_76]. **Figure 10** shows the median spread calculated in ten minute intervals for these four sites together with a metric of variation: the median absolute deviation divided by the square root of the number of decodes in each interval. Previous studies [e.g. 5] have shown that frequency spread of less than 100 mHz is associated with one-hop propagation. Furthermore, when one-hop propagation prevails, the variation in frequency spread is generally low, of order tens of milliHertz. The two ten-minute intervals most affected by excess absorption, centred on 18:05 and 18:10 UTC showed both these characteristics of one-hop propagation. The other points suggest this was a time of day and frequency that supported both one- and two-hop propagation, with one-hop dominating at 17:25 and 17:45 UTC and two-hop at other times.

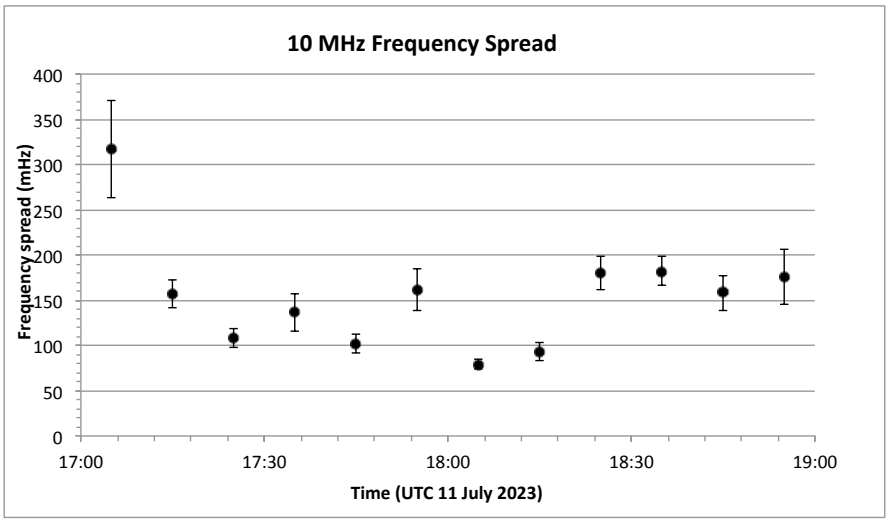

Figure 10. Median frequency spread in ten minute intervals of FST4W-120 transmissions at 10 MHz for sites at a ranges of 1137 km to 1234 km [NUT KIWI1, KFS Omni_C, KFS NW, KPH HF_76] showing a collective minimum centred at 18:05 UTC. The error bars denote the median absolute deviation divided by the root of the number of decodes [16 to 20].

It is fair to conclude that these frequency spread measurements do show that two-hop propagation, with its additional excess absorption, was suppressed during the core of the event from 18:00 to 18:20 UTC.

7. Comparing measured oblique excess absorption with the NOAA/SWPC model

An estimate of the absorption on oblique paths through the ionosphere can be derived from the vertical value using Martyn's 1935 absorption theorem [9]. It has limitations: strictly it applies only on a plane earth with a plane ionosphere and with no magnetic field. Despite these limitations the theorem is still used, e.g. in a solar flare study by Levine et al. [3]. It states:

$$A_{oblique}(f) = 2\cos(90^\circ - \varphi_{el}) A_{vertical}(f\cos(90^\circ - \varphi_{el}))$$

where $A_{vertical}$ is the model absorption at the frequency given by the operating frequency f times the cosine function including the ray elevation angle φ_{el}. There is a further assumption that both frequencies would be reflected from the same height. The factor two is for one-hop propagation, that is, two transits of the ionosphere.

From the 10 MHz data set, taking KPH as the most complete record, the excess absorption was 28.5 dB. From a PyLap ray trace simulation the ray elevation angle for the 1154 km one-hop path from WB6CXC was 26°. This gives a model-derived oblique path estimate of 21.7 dB, 7 dB lower than measured. Many researchers have found the values calculated from Martyn's theorem to be too low, e.g. Yagnik et al. and references therein [10].

References

1. https://turnislandsystems.com/meet-the-beaconblaster-6/
2. https://hamsci.org/eclipse
3. e.g. Levine, E.V., Sultan, P.J. and Teig, L.J., 2019. A parameterized model of X-ray solar flare effects on the lower ionosphere and HF propagation. *Radio Science*, *54*(2): 168-180.
4.https://spaceweather.com/images2023/11jul23/blackoutmap.jpg
5. Griffiths, G., 2023 Insights into HF propagation using FST4W. *RSGB RadCom* 99(9): 30-32.
6. http://wsprdaemon.org/ and http://wsprdaemon.org/timebasedb.html
7. https://using.tech/posts/fst4/
8. https://github.com/hamsci/pylap
9. Martyn, D. F., 1935. The propagation of medium radio waves in the ionosphere. *Proceedings of the Physical Society* 47(2): 323.
10. Yagnik, H.K., Acharya, B.L., Rai, R.K., Sharma, R.C., Mathur, I.C. and Sharma, K.D., 1984. Ionospheric Absorption at Vertical & Oblique Incidence at Low Latitudes. *Indian Journal of Radio and Space Physics* 13 (June): 94-97.